Inorganic Chemistry

Article

pubs.acs.org/IC

Photophysical Studies of Bioconjugated Ruthenium Metal–Ligand Complexes Incorporated in Phospholipid Membrane Bilayers

Ayesha Sharmin,[†] Luca Salassa,[‡,§] Edward Rosenberg,*[,†] J. B. Alexander Ross,*[,†] Geoffrey Abbott,[†] Labe Black,[†] Michelle Terwilliger,[†] and Robert Brooks[†]

[†]Department of Chemistry and Biochemistry, University of Montana, Missoula, Montana 59812, United States

[‡]CIC biomaGUNE, Paseo Miramón 182, 20009, Donostia–San Sebastián, Spain

Supporting Information

ABSTRACT: The luminescent, mono-diimine ruthenium complexes $[(H)Ru(CO)(PPh_3)_2(dcbpy)][PF_6]$ (**1**) (dcbpy = 4,4′-dicarboxy-2,2′-bipyridyl) and $[(H)Ru(CO)(dppene)(5\text{-amino-1,10-phen})][PF_6]$ (**2**) (dppene = bis(diphenylphosphino)-ethylene; phen = phenanthroline) were conjugated with 1,2-dihexadecanoyl-*sn*-glycero-3-phosphoethanolamine (DPPE) and with cholesterol in the case of complex **2**. Using standard conjugation techniques, compound **1** gives the bis-lipid derivative $[(H)Ru(CO)(PPh_3)_2(dcbpy\text{-}N\text{-}DPPE_2)][PF_6]$ (**3**), while **2** provides the monolipid conjugate [(H)Ru(CO)(dppene)-(1,10-phen-5-NHC(S)-*N*-DPPE)][PF_6] (**4**) and the cholesterol derivative [(H)Ru(CO)(dppene)(1,10-phen-5-NHC(O)-Ocholesteryl)][PF_6] (**5**). These compounds were characterized by spectroscopic methods, and their photophysical properties were measured in organic solvents. The luminescence of lipid conjugates **3** and **4** is quenched in organic solvents while compound **4** shows a weak, short-lived, blue-shifted emission in aqueous solution. The cholesterol conjugate **5** shows the long-lived, microsecond-time scale emission associated with triplet metal-to-ligand charge-transfer excited states. Incorporation of conjugate **3** in lipid bilayer vesicles restores the luminescence, but with blue shifts (~80 nm) accompanied by nanosecond-time scale lifetimes. In the vesicles conjugate **4** shows a short-lived and blue-shifted emission similar to that observed in solution but with increased intensity. Conjugation of the complex $[(H)Ru(CO)(PhP_2C_2H_4C(O)O\text{-}N\text{-succinimidyl})_2(bpy)][PF_6]$ (**6″**) (bpy = 2,2′-bipyridyl) with DPPE gives the phosphine-conjugated complex $[(H)Ru(CO)(PhP_2C_2H_4C(O)\text{-}N\text{-}DPPE)_2(bpy)][PF_6]$ (**7**). Complex **7** also exhibits a short-lived and blue-shifted emission in solution and in vesicles as observed for complexes **3** and **4**. We have also conjugated the complex $[Ru(bpy)_2(5\text{-amino-1,10-phen})][PF_6]_2$ (**8**) with both cholesterol (**9**) and DPPE (**10**). Neither complex **9** nor the previously reported complex **10** exhibited the blue shifts observed for complexes **3** and **4** when incorporated into large unilamellar vesicles (LUVs). The anisotropies of the emissions of complexes **3**, **4**, and **7** were also measured in LUVs, and those of complex **5** were measured in both glycerol and LUVs. High fundamental anisotropies were observed for complexes **3**, **4**, and **7**.

INTRODUCTION

The objective of this study is to synthesize probes suitable for incorporation into biological membranes for membrane dynamics measurements. To achieve this objective, we have synthesized a series of luminescent probes derived from ruthenium-based metal complexes that are tethered either to lipids or to cholesterol and have long excited-state lifetimes and low molecular symmetry.

The diffusion dynamics of proteins and protein assemblies that associate with membrane bilayers are slow, on a time scale of microseconds and longer, compared to the rotational diffusion of proteins in solution, which occurs on a time scale of several to tens of nanoseconds.[1] For example, the correlation times of the rotational motions of membrane-bound proteins can be microseconds to milliseconds.[2−5] The difference in time scales for these dynamical processes (microseconds versus tens of nanoseconds) is the result of interactions between the proteins and the membrane lipids. The fluorescence probes most useful for studying protein dynamics in solution have excited-state lifetimes in the range of 5−30 ns. Longer excited-state lifetimes are needed to measure the dynamics of biomacromolecules on or in membranes. Microsecond and millisecond time scale dynamics are often studied by using phosphorescent probes.[6−8] Other techniques, such as electron paramagnetic resonance (EPR), using site-directed spin labeling are also useful for these purposes.[9] However, excited-state probes potentially offer greater sensitivity for signal detection when compared with EPR.

Transition-metal complexes containing one or more diimine ligands exhibit tunable, long luminescence lifetimes (100 ns to ~10 μs), polarized emission, high photostability, large Stokes shifts, and sensitivity to the probe environment.[10,11] In addition, the lifetimes of these probes can be tuned by varying the ligands attached to the metal center.[11,12] Microsecond excited-state

Received: March 21, 2013
Published: September 24, 2013

lifetimes and polarized emissions make them useful probes for studying the microsecond time scale dynamics of membranes and macromolecular assemblies.

$[Ru^{II}(bpy)_3]^{2+}$ and other similar transition-metal complexes are now extensively used to understand the nature of the charge-transfer excited state.[2,3,13−17] Typically these complexes contain diimine ligands such as 2,2′-bipyridyl (bpy), 1,10-phenanthroline (phen), and their derivatives 4,4′-dicarboxy-bpy (dcbpy) and 5-amino-1,10-phen, which provide low-energy π^* orbitals for accepting the excited electron from the metal. Other ligands, such as phosphines, carbonyl, and halides, can be introduced with the diimine ligands to tune the luminescence and solution properties. In these systems, the initial singlet excited state undergoes intersystem crossing with a quantum efficiency close to unity; the radiative lifetime of the triplet metal-to-ligand charge transfer (^{3}MLCT) state reflects the effect of strong spin−orbit coupling on the degree of singlet−triplet mixing in the excited state.[18,19] As a result, the luminescence lifetime and the overall emission quantum yield of these complexes depend only on the radiative (k_r) and nonradiative (k_{nr}) decay rates of the triplet state. According to the energy gap law, k_{nr} increases exponentially as the emission energy decreases.[20−23] Other factors, such as the Jahn−Teller distortion of the excited ^{1}MLCT state, also increase nonradiative decay (k_{nr}).[24−26] Therefore, in order to obtain luminescence from transition-metal complexes, a delicate balance the energy levels of the metal and the ligand energy levels must be established.

The highly polarized emission from some of these complexes stimulated our interest in using these complexes as anisotropy probes for biophysical studies.[9,27] Luminophores covalently attached to macromolecules often undergo local (segmental) motions in addition to depolarization through global Brownian tumbling of the entire macromolecule. This results in complex anisotropy decays; time-resolved anisotropy measurements can be used to resolve information about segmental motion, global motion, size and shape of the macromolecule, and flexibility of the system.[5] From a practical point of view, the fundamental, zero-time anisotropy (r_0) should be at least 0.05 or greater.

The fundamental anisotropy is related to molecular symmetry. For example, $[Ru^{II}(bpy)_2(dcbpy)]^{2+}$ and $[Ru^{II}(bpy)_2(phen)]^{2+}$, which contain more than one type of diimine ligand, (i.e., less symmetric), show higher maximum fundamental anisotropies (excited near 490 nm, r_0 ∼0.25 and ∼0.175, respectively) than the more symmetric complex $[Ru(bpy)_3]^{2+}$ (excited near 460 nm, r_0 ∼0.13).[5] Transition-metal complexes with a single chromophoric ligand have been reported for Re(I) and Ru(II) complexes (e.g., $[Re(4,7\text{-}Me_2\text{-}phen)(CO)_3(4\text{-}COOHPy)][PF_6]$[28] and $[(H)Ru(CO)(dcbpy)(PPh_3)_2][PF_6]$[11]), but their fundamental anisotropies have not been reported. Because low molecular symmetry is expected to promote high anisotropy, and because high anisotropy is required for membrane dynamics measurements, the complexes reported here were designed with one diimine ligand, the anisotropy of which is compared in one case with a that of a tris-diimine complex.

Covalently attaching a ruthenium−polypyridyl probe with a long-lived excited state to either cholesterol or a phospholipid requires complementary functional groups for conjugation. Metal−polypyridyl complexes with carboxylate or amine functional groups are suitable for covalent conjugation to lipids, cholesterol, and proteins.[5,9,29] Phosphatidylethanolamine, a glycerophospholipid found in biological membranes, contains an amine group that can be reacted with a carboxyl group on the metal ligand via formation of an activated ester. The chloroformate derivative of cholesterol, on the other hand, can be covalently bound to an amine-substituted ligand. In both cases, the resulting conjugates can be easily incorporated into lipid-bilayer vesicles or biological membranes for photophysical measurements.[2,17]

Here, we report phospholipid and cholesterol conjugates for the complexes $[(H)Ru(CO)(PPh_3)_2(dcbpy)][PF_6]$ (**1**) and $[(H)Ru(CO)(dppene)(5\text{-amino-}1,10\text{-phen})][PF_6]$ (**2**), (dppene = bis(diphenylphosphino)ethylene), along with a detailed analysis of their polarized emissions when they are incorporated into different types of large lipid unilamellar vesicles (LUVs). To understand the effects of conjugation through the diimine luminophore on the photophysical properties of these complexes, we also present an investigation of the first example of an transition-metal complex conjugated through the phosphine ligand using *trans*-$[(H)Ru(bpy)(Ph_2PCH_2CH_2COOH)_2][PF_6]$ (**6′**) as the precursor. To our knowledge, this is the first such report. For comparison with the photophysical properties of the phosphine-containing complexes **1**−**6′**, we also report the photophysical properties of the cholesterol and monolipid conjugates of the complex $[Ru(bpy)_2(5\text{-amino-}1,10\text{-phen})][PF_6]_2$ (**8**). The lipid conjugate of complex **8** was previously reported.[17]

EXPERIMENTAL SECTION

General Methods and Materials. The reactions were carried out under nitrogen. Purification was carried out in air by using preparative thin-layer chromatography (10 × 20 cm plates coated with 1 mm silica gel PF 60254-EM Science). Activated neutral alumina (Aldrich, 150 mesh, 58 Å) was also used to purify compounds by column chromatography. Reagent-grade solvents were purchased from J.T. Baker. Methylene chloride (CH_2Cl_2) and acetonitrile (MeCN) were distilled from calcium hydride. Tetrahydrofuran (THF) was distilled from benzophenone ketyl. Ruthenium carbonyl was purchased from Strem Chemicals. Cholesteryl-chloroformate, thiophosgene, 1,10-phen, 5-amino-1,10-phen, bpy, and dcbpy were purchased from Sigma-Aldrich and used as received. 1,2-Dihexadecanoyl-*sn*-glycero-3-phosphoethanolamine (DPPE), 1,2-dihexadecanoyl-*sn*-glycero-3-phosphocholine (DPPC), 1,2-dimyristoyl-*sn*-glycero-3-phosphocholine (DMPC), and L-α-phosphatidylcholine from chicken egg (egg-PC) were purchased from Avanti Polar Lipids Inc. and used as received. The complexes $[(H)Ru(CO)(PPh_3)_2(dcbpy)][PF_6]$ (**1**) and $[(H)Ru(CO)(dppene)(5\text{-amino-}1,10\text{-phen})][PF_6]$ (**2**) were synthesized according to published procedures.[11] The compounds $[Ru(bpy)_2(5\text{-amino-}1,10\text{-phen})][PF_6]_2$ (**8**) and $[Ru(bpy)_2(1,10\text{-phen-}5\text{-NHC(S)-}N\text{-DPPE})][PF_6]_2$ (**10**) were synthesized according to literature procedures.[17b] ^{1}H NMR and $^{31}P\{^1H\}$ NMR spectra were obtained on a Varian 400 MHz Unity Plus or a Varian NMR Systems 500 MHz spectrometer. Fourier transform infrared (FT-IR) spectra were obtained on a Thermo-Nicolet 633 FT-IR spectrometer. Electrospray ionization mass spectrometry (ESI-MS) spectra were obtained on a Waters Micromass LCT using 80% MeCN as the carrier solvent.

Luminescence Spectroscopy. Steady-state UV−visible absorption spectra and emission spectra were recorded on a Molecular Device Spectra Max M2. The emission quantum yields (φ) for the ruthenium complexes in the presence of oxygen were calculated relative to a Rhodamine B standard (φ = 0.73, in ethanol).[11,30a]

$$\varphi = \frac{\text{abs Rhodamine B}}{\text{area Rhodamine B}} \times \frac{\text{area Ru complex}}{\text{abs Ru complex}} \quad (1)$$

Here "abs" refers to the absorbance of the luminophores at the excitation wavelength, and "area" refers to the integrated area under the emission spectral curve. In the case of compound **7** the quantum yield was measured by a similar procedure, but because of the blue-shifted emission of this complex, fluorescein was used as the standard.[30b] Details of the methods used for the time-resolved spectroscopy are given in the Supporting Information.[31−34]

dx.doi.org/10.1021/ic400706u | *Inorg. Chem.* 2013, 52, 10835−10845

Synthesis (see Schemes 1−3). *Synthesis of (H)Ru(CO)-(PPh$_3$)$_2$(dcbpy-N-succinimidyl)[PF$_6$] (**1′**).* A mixture of compound **1**[11] (155 mg, 0.16 mol) and *N*-hydroxysuccinimide (34 mg, 0.32 mmol) was stirred in 4 mL of dry MeCN at room temperature in a 10 mL round-bottom flask until all the reactants dissolved. *N*,*N*′-Dicyclohexylcarbodiimide (DCC) (103 mg, 0.48 mmol) was added to the mixture, and the reaction was stirred for three hours. The resulting solid precipitate (dicyclohexylurea) was removed by filtration through a 0.2 μm syringe filter. The filtrate was added to 5 mL of isopropanol, and the mixture was kept at −4 °C to complete the precipitation. The supernatant was evaporated, and the remaining orange residue was washed three times with 2 mL aliquots of dry ethyl ether. Compound **1′** was obtained in 32% yield (60 mg). IR in KBr: CO stretching frequency at 1956 (vs), 1775 (m), 1742 (s), 1650 (m) and CH aliphatic 2980 cm^{-1}. ^{1}H NMR (CDCl$_3$ δ): 9.6−7.2 (m, 36H), −11.1 (t, 1H), 2.8 (4H). ^{31}P{^{1}H} NMR (CDCl$_3$ δ): 49.2 (s, 2P), −155 (m, 1P).

*Synthesis of [(H)Ru(CO)(PPh$_3$)$_2$(dcbpy-N-DPPE$_2$)][PF$_6$] (**3**).* DPPE (30 mg, 0.043 mmol) was dissolved in CHCl$_3$, and 3.5 mL of triethylamine was added to the solution. The mixture was stirred for 15 min, and then a solution of complex **1′** (60 mg, 0.021 mmol) in 2 mL of dry MeCN was added dropwise over 20 min. The reaction was stirred overnight, and then the solvent was removed by rotary evaporation. The residue was purified by thin layer chromatography on silica gel. Two successive elutions with a mixture of hexane/methylene chloride/ethanol {6.5:3.5:0.5 (v/v)} yielded two bands. The baseline contained unreacted complex **1′**. The faster-moving UV-absorbing band was identified as unreacted DPPE, and the slower-moving deep yellow band gave compound **3** in 15% yield (22 mg). IR in KBr: CO stretching frequency at 1956 (vs), 1734 (s), 1684 (vs) and CH aliphatic 2963 (s), 2924 (s), 2851 (m) cm^{-1}. ^{1}H NMR (CDCl$_3$ δ): 9.5−7.0 (m, 36H), 5.2 (2H), 5.1−2.2 (35H), 1.9−0.78 (107H), −11.19 (br, 1H); ^{31}P{^{1}H} NMR (CDCl$_3$ δ): 49.6 (s, 2P), 25.04 (2P), −155 (m, 1P). ESI-MS: m/z 2034 [M$^+$ − (C$_{15}$H$_{31}$ + PF$_6$)] (calcd M$^+$ − (C$_{15}$H$_{31}$ + PF$_6$) = 2034).

*Synthesis of [(H)Ru(CO)(dppene)(1,10-phen-5-NCS][PF$_6$] (**2′**).* A 122 mg (0.13 mmol) sample of compound **2**[11] was dissolved in 3 mL of dry acetone. Finely crushed CaCO$_3$ (45 mg, 0.45 mmol) was added to the solution of complex **2** followed by addition of thiophosgene (11 μL, 0.07 mmol). The reaction mixture was stirred at room temperature for 1 h and then refluxed for 2.5 h. After the mixture was cooled to room temperature, CaCO$_3$ was removed by using a 0.45 μm filter, and the acetone was removed by rotary evaporation. Compound **2′** was obtained in 94% yield (50 mg). IR in KBr: CO stretching frequency at 1990 (vs), N═C═S at 2119 (m) and 2046 (m) cm^{-1}. ESI-MS: m/z 860 [M$^+$ − PF$_6$] (calcd M$^+$ − PF$_6$ = 860).

*Synthesis of [(H)Ru(CO)(dppene)(1,10-phen-5-NHC(S)-N-DPPE]-[PF$_6$] (**4**).* A solution of compound **2′** (50 mg, 0.049 mmol in 3 mL of dry CH$_2$Cl$_2$) was added dropwise into a stirring solution of DPPE (35 mg, 0.048 mmol in 5 mL of dry CH$_2$Cl$_2$) over 1 h at room temperature, and the reaction was stirred overnight. The solvent was removed by rotary evaporation, and the residue was purified by thin-layer chromatography on silica plates. Three bands were resolved by elution with hexane/methylene chloride/methanol {3:6:2 (v/v)}. The fastest-moving UV-absorbing band was identified as unreacted DPPE, and the second moving yellow band was too small for further characterization. The slowest-moving, deep-yellow band yielded compound **4** in 10% yield (15 mg). IR in KBr: CO stretching frequency at 1993 (vs), 1735 (vs), cm^{-1}; NH stretching at 3422 and aliphatic C−H stretching at 2920 (vs), 2849 (vs) cm^{-1}. ^{1}H NMR (CDCl$_3$ δ): 7.5−6.6 (m, 29H), 5.32 (s, br 1H), 4.0−3.4 (m, 9H), 2.9−0.2 (63H), −7.80 (1H). ^{31}P{^{1}H} NMR (CDCl$_3$ δ): 68.30 (s, 2P), 58.19 (br, 1P), −145 (m, 1P).

*Synthesis of [(H)Ru(CO)(dppene)(1,10-phen-5-NHC(O)OChol)]-[PF$_6$] (**5**) (Chol = cholesteryl).* In 15 mL of dry CH$_2$Cl$_2$ and 1 mL of dry MeCN, 100 mg (0.10 mmol) of compound **2** was dissolved, and then 1 mL of triethylamine was added to the deoxygenated solution. A 10 mL CH$_2$Cl$_2$ solution of cholesteryl-chloroformate (45 mg, 0.10 mmol) was added to the probe solution dropwise over 20 min, and the mixture was refluxed for 5 h. Progress of the reaction was monitored by the disappearance of the peak at 1776 cm^{-1} in the IR spectrum, corresponding to the chloroformate, and by the appearance of a new peak at 1730 cm^{-1}, corresponding to the amide. The solvent was removed by rotary evaporation, and the residue was purified by thin layer chromatography on silica gel. Elution with hexane/methylene chloride/methanol {1:1:1 (v/v)} yielded two bands. Compound **5** was recovered in 20% yield (30 mg) from the orange, slower-moving band while the faster UV-absorbing band contained unreacted cholesteryl-chloroformate. IR in KBr: CO stretching frequency at 1997 (vs), 1976 (vs), 1735 (s), and CH aliphatic 3054 (w), 2926 (vs), 2850 (s) cm^{-1}. ^{1}H NMR (CDCl$_3$ δ): 8.5−6.5 (m, 29H), 6.05 (2m, 1H), 4.3 (s, 1H), 2.0−0.5 (44 H), −7.90 (m, 1H). ^{31}P{^{1}H} NMR (CDCl$_3$ δ): 75.71 (s, 2P), −145 (m, 1P).

*Synthesis of [(TFA)$_2$Ru(CO)$_2$(PPh$_2$C$_2$H$_4$C(O)OH] (TFA = Trifluoroacetic Acid) (**6**).* A THF solution of K[Ru(CF$_3$CO$_2$)$_3$(CO)$_3$][11] (500 mg, 0.90 mmol) and 3-(diphenylphosphino)propionic acid (DPPA) (425 mg, 1.8 mmol) was heated overnight at 45 °C. The solvent was removed by rotary evaporation, and the residue was vacuum dried yielding 625 mg (81%) of complex **6** as a pale yellow solid. IR in KBr: 2023 (vs), 2010 (vs), 1960 (m), 1790 (m, br), 1685 (vs, br) cm^{-1}. ^{1}H NMR in acetone-d_6: δ 7.9−7.3 (m, 20H), 3.90 (m, 2.8H, isomer a), 3.14 (m, 1.2H, isomer b), 2.57 (m, 1.2H, isomer b), 2.10 (m, 2.8H, isomer); ^{31}P{^{1}H} NMR: δ 26.59 (d, t, br).

*Synthesis of [(H)Ru(CO)(PPh$_2$C$_2$H$_4$C(O)OH)$_2$(bpy)][PF$_6$] (**6′**).* The reaction of complex **6** (300 mg, 0.35 mmol) with bpy (55 mg, 0.35 mmol) in ethylene glycol (15 mL) was heated at 140 °C for 72 h producing an orange solution. A deep-orange precipitate was obtained by the addition of NH$_4$PF$_6$ in deionozed (DI) water (1.0 g/10 mL) dropwise until precipitation was completed. The precipitate was filtered and washed three times with cold DI water, three times with diethyl ether, and dried under vacuum. Complex **6′** was obtained in 41% yield (135 mg). IR in KBr: 1971 (vs), 1730 (s), 1740 (vs), 1605 (s) cm^{-1}. ^{1}H NMR in acetone-d_6: δ 8.38−6.95 (m, 28H), 3.99 (t, 4H), 3.61 (t, 4H), −11.1 (t, 1H); ^{31}P {^{1}H} NMR: δ 43.06 (s, 2P), −145 (m, 1P).

*Synthesis of [(H)(CO)Ru(PPh$_2$C$_2$H$_4$C(O)-N-succinimidyl)$_2$(bpy)]-[PF$_6$] (**6″**).* The succinimidyl derivative was obtained by dissolving complex **6′** (100 mg, 0.106 mmol) in 5 mL of MeCN in a round-bottom flask at 0 °C along with *N*-hydroxysuccinimide (25 mg, 0.212 mmol) and DCC (65 mg, 0.32 mmol) overnight. After it was stirred, the reaction mixture was passed through a 0.2 μm syringe filter to remove urea that had precipitated. The filtrate was added to an excess of cold isopropanol and recrystallized. The resulting precipitate was filtered and washed three times with diethyl ether. Complex **6″** was obtained in 58% yield (70 mg, 0.061 mmol). IR in KBr: CO stretching frequency at 1939 (s), 1780 (s), 1736 (vs) and CH aliphatic 2930 (vs), 2853 (s) cm^{-1}. ^{1}H NMR (CDCl$_3$ δ): 8.6−6.7 (28H), 4.3−3.2 (8H), 2.95−2.8 (t, 8H), −11.3 (t, 1H). ^{31}P{^{1}H} NMR: δ 35.4 (2P) and −145 (1P).

*Synthesis of [(H)(CO)Ru(PPh$_2$C$_2$H$_4$C(O)-N-DPPE)$_2$(bpy)][PF$_6$] (**7**).* A MeCN solution of complex **6″** (60 mg, 0.048 mmol) was added dropwise into a stirring methylene chloride solution of DPPE (68 mg, 0.096 mmol) in the presence of a catalytic amount of triethylamine. The reaction mixture was stirred overnight at ambient temperature. The solvent was removed on a rotary evaporator, and the residue was purified by thin-layer chromatography on silica. Elution with hexane/methylene chloride/methanol (6:3:1) on silica gave a slower-moving yellow band and a faster-moving UV band with a heavy yellow baseline. The yellow compound on the baseline and the UV-absorbing band were identified as unreacted complex **6″** and DPPE, respectively. The yellow band on the TLC plate gave compound **7** in 20% (∼20 mg) yield. IR in KBr: CO stretching frequency at 1941 (s), 1735 (vs), 1653 (m) and CH aliphatic 2960 (s), 2918 (vs), 2850 (s) cm^{-1}. ^{1}H NMR (CDCl$_3$ δ): 8.6−6.7 (28H), 5.2−3.2 (44H), 3.0−0.4 (108H), −11.1 (t, 1H). Peaks in both the aliphatic and the aromatic regions were broad. The ^{31}P NMR showed that the phosphine peak and the phosphate peak of the lipid were also broad and appeared at δ 37.94 (2P) and 22.5 (2P), respectively; the PF$_6$ peak was at δ −145 (1P).

*Synthesis of [Ru(bpy)$_2$(1,10-phen-5-NHC(O)OChol)][PF$_6$]$_2$ (**9**).* Complex **8** was prepared according to a published method.[39] Complex **8** (100 mg, 0.11 mmol) was dissolved in 10 mL of dry CH$_2$Cl$_2$, and then 1 mL of triethylamine was added to the deoxygenated solution. A 5 mL CH$_2$Cl$_2$ solution of cholesteryl-chloroformate (50 mg, 0.11 mmol) was added to the probe-containing solution dropwise over 20 min, and the

dx.doi.org/10.1021/ic400706u | *Inorg. Chem.* 2013, 52, 10835−10845

reaction mixture was refluxed for 4 h. Progress of the reaction was monitored by the disappearance of the peak at 1776 cm^{-1} in the IR spectrum, corresponding to the chloroformate, and by the appearance of a new peak at 1731 cm^{-1}, corresponding to the amide. The solvent was removed by rotary evaporation, and the residue was purified by thin layer chromatography on silica gel. Elution with the solvent mixture hexane/methylene chloride/methanol {1:2:1 (v/v)} yielded two bands. The complex **9** was recovered in 14% yield (23 mg) from the orange, slower-moving band while the faster, UV-absorbing band contained unreacted cholesteryl-chloroformate. IR (KBr) (υ cm^{-1}): CO stretching frequency at 1731 (s) and CH aliphatic 3139 (w), 2950 (vs), 2868 (s). ^{1}H NMR ($CDCl_3$ δ): 8.7−7.0 (24H), 5.37 (1H), 3.99 (1H), 2.0−0.5 (43 H).

LUV Preparation. A chloroform mixture of the conjugated probe (**3**, **4**, **5**, or **7**) and DPPC, DMPC, or a mixture of phospholipids containing a choline headgroup (egg-PC) was prepared in a molar ratio of 1:99. The organic solvent was removed by evaporation with argon gas, and the lipid/chromophore mixture was further dried under vacuum overnight. Then 0.52 mL of saline buffer (20 mM *N*-(2-hydroxyethyl)piperazine-*N*′-ethanesulfonic acid, 100 mM NaCl, pH 7.5) was added to the dried lipid, and the solution was maintained above the phase-transition temperature of the corresponding phosphocholine (41 °C for DPPC, 23 °C for DMPC, and less than 0 °C for egg-PC)[34] to obtain a final lipid concentration of 1 mM. Addition of the buffer to the lipid mixture produced cloudy suspensions. The suspensions were incubated above the phase-transition temperature for 1 h with occasional stirring. Then a freeze/thaw cycle was carried out 5 times. Finally, clear suspensions of ∼100 nm diameter LUVs were obtained by extrusion through a 100 nm sizing membrane as previously described.[35]

RESULTS

Synthesis. Schemes 1 and 2 describe the ligand modification and conjugation of the ruthenium probes with lipids and cholesterol. For the phospholipid conjugations, we used diimine ligands containing either activated ester or highly reactive isothiocyanate functional groups. Complex **1** contains a bpy ligand with two carboxylic acid groups, which were converted to the activated ester groups, and the activated ester groups were then used to form a peptide bond with the primary amine of DPPE. Complex **3**, conjugated to two DPPE molecules, was synthesized and purified by standard chromatographic methods. Complex **4** was obtained by first converting the amine group on the 5-amino-1,10-phen ligand of complex **2** into 5-isothiocyanato-1,10-phen (SCN-phen), and then one molecule of DPPE was conjugated with the ruthenium probe through formation of a thiourea bond between SCN-phen-Ru and the primary amine group of DPPE. Because cholesterol is an important component of biological membranes, we synthesized the cholesterol conjugate of the ruthenium complex **2**. The amino group of 5-amino-1,10-phen was used to form the amide bond in complex **5** by reacting complex **2** with the highly reactive cholesteryl-chloroformate.

Scheme 1

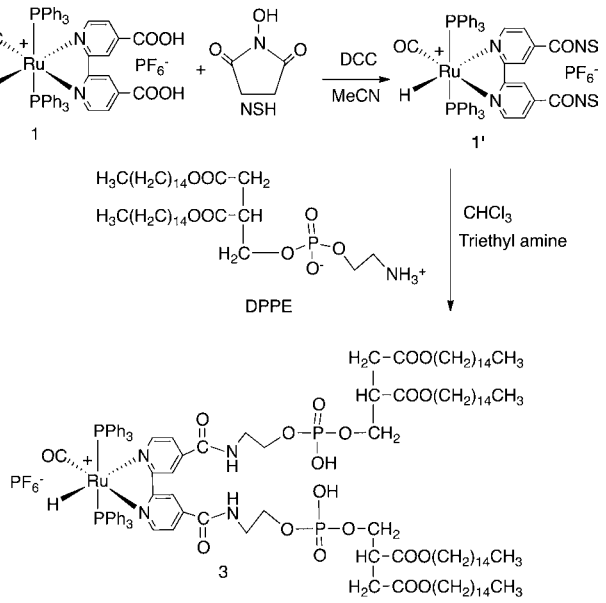

DPPE =1,2-dihexadecanoyl-sn-glycero-3-phosphoethanolamine
NHS = N- hydroxy succinimide
DCC = dicyclohexyl carbodiimide

All conjugated transition-metal complexes reported here were characterized by IR, ^{1}H NMR, and ^{31}P NMR spectroscopies. In the IR, the terminal M−CO shows CO stretching modes around 2150−1850 cm^{-1}. Complexes **1**−**5** have only one M−CO ligand. The strong M−CO stretch appears at 1949 and 1956 cm^{-1} for complexes **1** and **3**, respectively, and complexes **2**, **4**, and **5** showed strong M−CO stretches from 1990 to 1997 cm^{-1}. Strong absorptions in the organic carbonyl region were also observed for the carboxy-amide functional group in complex **5** and for the glycero-ester groups of lipids in complexes **3** and **4**. Medium intensity absorptions from 2102 to 2050 cm^{-1} are observed for **4**, which are assignable to the iso-thiocyanate (N═C═S) stretches.

The ^{1}H and ^{31}P{^{1}H} NMR spectra of complexes **1**′ and **3** obtained in $CDCl_3$ are consistent with the proposed structures. The M−H resonance appeared as a triplet at δ −11.07 (J = 20 Hz) for complex **1**′ and as a broad multiplet at δ −11.19 upon conjugation with lipids in complex **3**. The hydride resonances for complexes **2**, **4**, and **5** appear as triplets at δ −7.61, −7.5, and −7.6, respectively. The aromatic region of the ^{1}H spectra is complex because of the phenyl protons of the phosphine ligands and the aromatic protons of the diimine ligands. The CH═CH protons of dppene are observed from δ 6.2 to 6.9 for complexes **2**, **4**, and **5**. The conjugates showed chemical shifts in the aliphatic regions that are characteristic of the corresponding lipid and cholesterol. The ^{1}H NMR resonances for the lipid and cholesterol conjugates are slightly broader than those of the unconjugated complexes (see Supporting Information Figures S6−S10), probably because the rotational correlation times of the complexes are long, which means that the molecules are not orientationally averaged and therefore do not display sharp signals. This could also be the result of aggregate formation in the polar organic solvents used.

The chemical shifts of the metal-bound phosphine ligands in the ^{31}P NMR spectra are in good agreement with those of similar Ru(II)phosphine complexes.[11] Complexes **1**−**5** show singlet resonances from δ 49.2 to 75.7 relative to external H_3PO_4; these resonances are due to the triphenyl and diphenylphosphinoethylene ligands. The singlet observed for these complexes indicates that they have a symmetry plane that makes the two phosphorus nuclei magnetically equivalent in complexes **1** and **3**, which is consistent with the proposed structures. That singlets are observed for complexes **3**−**5** as well suggests that the asymmetry in the phenanthroline ring is not sufficient to preclude overlap of the phosphine resonances. This is also the case for complex **2**.[11] The ^{31}P resonances for the lipid phosphorus atoms are observed at δ 25.0 (2P) and 58.19 (1P) for complexes **3** and **4**, respectively. The higher-frequency shift in complex **4** relative to that of complex **3** might result from the different modes of binding to the diimine ring or to conformational effects.

dx.doi.org/10.1021/ic400706u | Inorg. Chem. 2013, 52, 10835−10845

Scheme 2

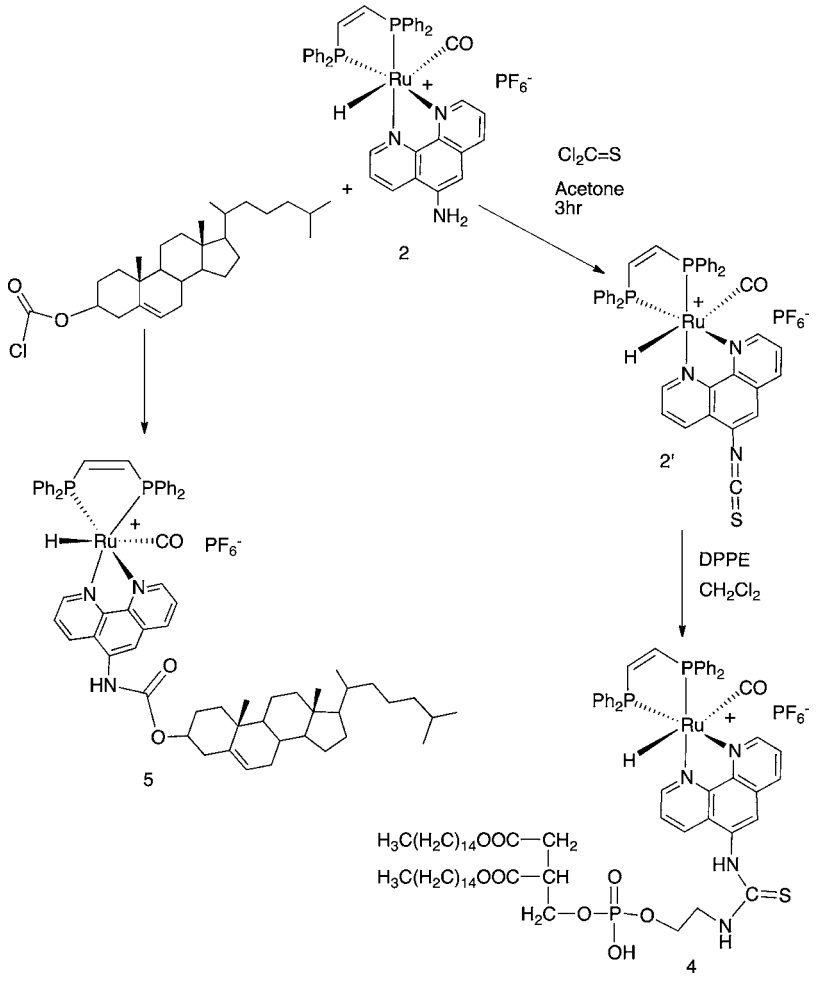

In all the ^{31}P NMR spectra, the counteranion [PF_6] appeared as a septet at δ −155 with an integrated relative intensity of 1:2 when compared with the phosphine ligand resonances.

To evaluate the effect of the site of lipid conjugation on the photophysical properties of the complexes in LUVs, we synthesized complex **7** (Scheme 3). This was done by reacting the common starting material [K][$Ru(CO)_3(TFA)_3$] with DPPA to give the 3-(diphenylphosphino)propionyl carboxylate **6** (two isomers were observed by ^{1}H NMR), which was then reacted with bpy to give complex **6′**. The bis-lipid conjugate was obtained by conversion of complex **6′** to the activated ester derivative **6″**. Then conjugation with DPPE, using a procedure similar to that used for the synthesis of complex **3**, gave *trans*-[(H)Ru-($PPh_2C_2H_4C$(O)-*N*-DPPE)$_2$(bpy)(CO)][PF_6] (**7**) (Scheme 3). The complexes were characterized spectroscopically at each stage of the synthesis, to confirm evidence of the formation of the expected analogues of complexes **1** and **3**. Under the conditions used for the reaction with bpy, namely, refluxing in ethylene glycol, all of the complexes were converted to their corresponding hydrides.

Note that complexes **4** and **5** are chiral, while complexes **3** and **7** are not, by virtue of the symmetry plane that is perpendicular to the two *trans*-phosphines and contains the other ligands. Because we observe only one set of NMR resonances for both complexes, either the chemical shift differences for the diastereomers of complexes **4** and **5** are not large enough to be resolved or only one of the diastereomers is populated.

Scheme 3

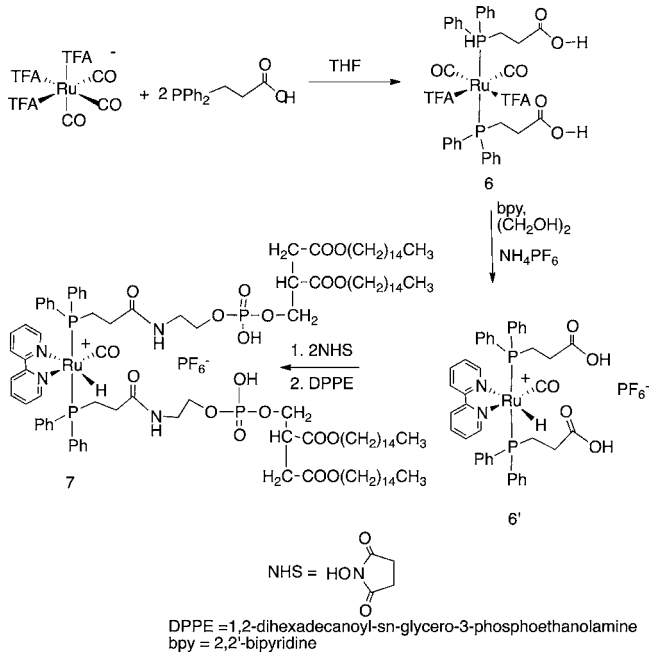

Photophysical Characterization of Complexes 1−5, 6′, and 7−10. Table 1 lists the absorption and emission maxima

dx.doi.org/10.1021/ic400706u | *Inorg. Chem.* 2013, 52, 10835−10845

and the luminescence lifetimes for complexes **1**−**7** in ethanol. All of the compounds show intense, higher-energy absorptions at 270−295 nm due to the spin-allowed intraligand ($\pi-\pi^*$) transitions. These absorptions are not shown in Table 1 in order

Table 1. Absorption, Emission, and Excited-State Lifetimes of Ruthenium MLCT Probes in Ethanol

compound	λ_{ab} (nm)	λ_{em} (nm)	τ (μs)	ϕ
1 [HRu(CO)$(PPh_3)_2$(4,4′-dcbpy)][PF_6]	303, 468	647	0.72	0.30[a]
2 [(H)Ru(CO)dppene)(5-amino-1,10-phen)][PF_6]	364, 442	610	0.25	0.25[a]
3 [HRu(CO)$(PPh_3)_2$(dcbpy-*N*-$DPPE_2$)][PF_6]	316, 442			
4 [(H)Ru(CO)(dppene)(1,10-phen-5-NHC(S)-*N*-DPPE)][PF_6]	360, 400	520		
5 [(H)Ru(CO)(dppene)(1,10-phen-5-NHC(O)OChol)][PF_6]	356, 440	605	0.47	0.49
6′ [(H)Ru(CO)$(dppa)_2$(bpy)][PF_6]	460	608	0.27	0.50[b]
7 [(H)Ru(CO)(dppa-*N*-$DPPE)_2$(bpy)][PF_6]	295, 400	505	0.004	0.019
8 [$Ru(bpy)_2$(5-amino-1,10-phen)][$PF_6]_2$	350, 445	625	0.22	
9 [$Ru(bpy)_2$(1,10-phen-5-NHC(O)OChol)][$PF_6]_2$	350, 445	625	0.22	0.25
10 [$Ru(bpy)_2$(1,10-phen-5-*N*-DPPE)][$PF_6]_2$[c]	330, 460	625	0.22	

[a]From ref 11. [b]This work. [c]From refs 17 and 39.

to focus on the more important MLCT and phosphine absorptions. In the case of complex **7** the absorption at 295 nm is due to the phosphine. The absorptions of this complex are all blue-shifted relative to the others including the MLCT (vide infra), and this is borne out by the excitation spectra (see Supporting Information Figure S1). The absorptions observed between 356 and 366 nm for complexes **2**, **4**, and **5** are due to the presence of the double bond in the chelating phosphine ligand of these complexes. The less-intense absorption bands ($\varepsilon_{450} \approx 2 \times 10^3$ M^{-1} cm^{-1}) of all probes and their conjugates in the visible region (410−490 nm) are attributed to spin-allowed ^{1}MLCT (d−π^*) transitions. The ^{1}MLCT absorption bands of the complexes containing dcbpy are at slightly lower energy than the lipid-derivative complex **3**. In the cases of complexes **4** and **7** the MLCT absorption is blue-shifted to ≈ 400 nm (see Supporting Information Figures S4 and S5).

All the complexes containing the chelating phosphine and phenanthroline ligands displayed ^{1}MLCT absorption bands at similar wavelengths. In ethanol, acetonitrile, or methylene chloride, complexes **1**, **2**, **5**, and **6′** displayed long-lived, orange-red luminescence characteristic of a ^{3}MLCT excited state (see Figure 1; the emission spectra of complexes **5** and **6′**—not shown—are very similar to those of complexes **2** and **1**, respectively). The conjugation with cholesterol (complex **5**) resulted in an approximate twofold increase of the excited-state lifetime. No emission was observed from complex **3**, and a very weak emission at 520 nm was observed for complex **4**. This emission had a short lifetime (4−5 ns) and had an ill-defined excitation spectrum (see Supporting Information, Figure S4). At 608 nm, complex **6′** exhibits a ^{3}MLCT emission, which interestingly has a much shorter lifetime but a higher quantum yield than that of complex **1**. Complex **7** showed a blue-shifted ^{1}MLCT absorption band with a peak near 400 nm; excitation at 450 nm gave an emission with a maximum at 505 nm with a lifetime of ∼4.46 ns in

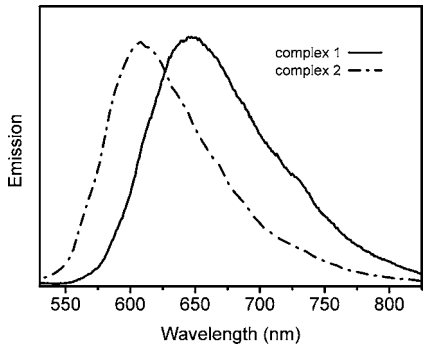

Figure 1. Peak-normalized emission spectra of complex [HRu(CO)$(PPh_3)_2$(dcbpy)][PF_6] (**1**) and [(H)Ru(CO)(dppene)(5-amino-1,10-phen)][PF_6] (**2**) in ethanol.

chloroform at 5 °C (see Table 1). The quantum yield of this emission was found to be 0.019, making this a very weak singlet emission. Thus, bis-lipid conjugation via the phosphine ligand does not cause quenching of the luminescence as seen for complex **3** but gives the short-lived, blue-shifted emission in ethanol observed for complex **4**. Complexes **8**−**10**, on the other hand, showed identical long-lived ^{3}MLCT emissions with a peak near 625 nm. The absorption and emission spectra of complex **9** are shown in Figure 2. Analysis of the time-resolved anisotropy

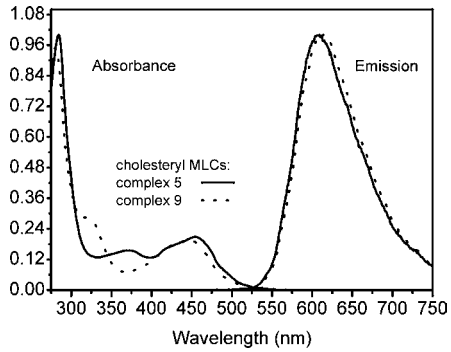

Figure 2. Absorption and emission spectra of complex [(H)Ru(CO)(dppene)(1,10-phen-5-NHC(O)OChol)][PF_6] (**5**) and complex [$Ru(bpy)_2$(1,10-phen-5-NHC(O)OChol)][$PF_6]_2$ (**9**) in ethanol.

decay of complexes **1**, **2**, and **5** in neat glycerol at 0 °C and with excitation at 470 nm yielded r_0 values of 0.124, 0.077, and 0.121, respectively.

Photophysical Studies of Complexes 3−5, 7, 9, and 10 Incorporated in Lipid Membrane Bilayers. The lipid conjugates **3**, **4**, **7**, and **10** and the cholesterol conjugates **5** and **9** were incorporated in LUVs to study the photophysical properties of these probes in a membrane-like environment. The maximum of the low-energy absorption band was near 440 nm except for complexes **4** and **7**, which had this absorption at ∼400 nm. The dynamics of these probes incorporated in the LUVs were determined from the kinetics of the time-resolved emission anisotropy. Although the absorption spectrum for complex **3** from 400 to 550 nm was characteristic of the charge-transfer band and essentially identical in chloroform, ethanol, and lipid LUVs, emission was only observed when complex **3** was incorporated in LUVs. Furthermore, the emission spectrum of complex **3** in the LUVs was blue-shifted (λ_{max} = 534 nm) with respect to that of the precursor probe **1** (λ_{max} = 647 nm in ethanol) (see Table 1 and Figure 1). Complex **3** also exhibited a

dx.doi.org/10.1021/ic400706u | *Inorg. Chem.* 2013, 52, 10835−10845

very short excited-state lifetime (11 ns at 5 °C, air equilibrated) in PC−LUVs. Complex **4** in ethanol solution showed a weak short-lived emission at 520 nm. Complex **4** in PC−LUVs also had a blue-shifted emission (545 nm) with a short lifetime (8 ns) (see Figure 3), similar to its emission in solution, but with a much

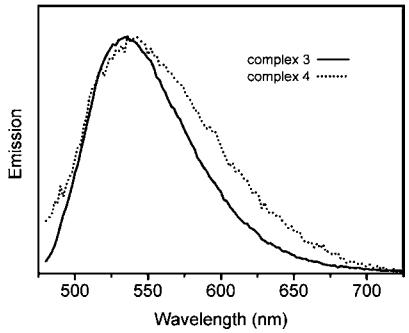

Figure 3. Peak-normalized emission spectra of complex [(H)Ru(CO)-$(PPh_3)_2$(dcbpy-*N*-$DPPE_2$)][PF_6] (**3**) and [(H)Ru(CO)(dppene)-(1,10-phen-5-NHC(S)-*N*-DPPE][PF_6] (**4**) in egg-PC−LUVs.

higher intensity. Both complexes showed more intense emission in LUVs compared to that of the red-shifted emission of the unconjugated precursors **1** and **2** in ethanol. The emission yield of complex **3** was greater than that of complex **4**, as was the case for the bpy complex **1** relative to the phen complex **2**. Complex **7** showed the same blue-shifted emission in the LUVs as in ethanol. Complex **10** did not show this blue shift when incorporated in LUVs but did show a factor of 2 increase in the excited-state lifetime (0.22 to 0.52 μs).

To eliminate the possibility that the blue-shifted, short-lifetime emissions of complexes **3** and **4** in lipid LUVs were due to decomposition in the lipid bilayer, we synthesized the bis-lipid derivative dcbpy-*N*-$DPPE_2$ (**11**) (see Supporting Information) and compared the photophysical behavior of this compound in egg-PC−LUVs to that of complexes **3** and **4** in lipid LUVs. This conjugate, which lacks the metal center, showed a less intense absorption band at 327 nm and an intense absorption band at 295 nm, characteristic of the unconjugated dcbpy ligand. Furthermore, the emission maximum of **11** in PC−LUVs was at 405 nm (excitation at 327 nm), not near 534 nm, and complex intensity decay kinetics were observed with a 5 ns intensity-averaged lifetime, $\langle\tau\rangle$. In another experiment, we prepared PC−LUVs without any probe incorporated. As expected, there was no emission whether excited at 327 or 450 nm. These LUVs, which lacked a probe, were then incubated at 35 °C with complex **3** previously dissolved in THF (THF was approximately 2% of the final volume) to *adsorb the probe onto* the LUVs. In contrast to the conjugate incorporated in LUVs by the standard reconstitution procedure, described previously, the emission spectrum of the bis-lipid conjugate *adsorbed* onto the preformed LUVs had its maximum at 620 nm, characteristic of ^{3}MLCT luminescence. However, when this preparation was subsequently extruded through the sizing membrane, the blue-shifted emission with a maximum near 530 nm was once again observed. These results indicate that the blue-shifted emission and short, nanosecond-time scale excited-state lifetime observed for complex **3** are not due to the decomposition of the complex to a free bpy-DPPE moiety, but are features of the system when the probe is incorporated into the LUV bilayer. This conclusion is also supported by the observation that the ^{1}MLCT absorption band of complex **3** is the same both in alcohol solution and in PC−LUVs.

A progressive decrease in the blue-shifted luminescence intensity with increasing temperature was observed over the temperature range of 5−50 °C (Table 2). The change in excited-state lifetime and the anisotropy decay of the blue-shifted emission of complexes **3** and **4** incorporated in PC−LUVs were also measured over a range of temperatures to determine the sensitivity of these probes toward changes in the microviscosity of the bilayer environment. The excited-state lifetime decreased progressively with increasing temperature, consistent with the decrease in luminescence expected for quenching by thermally activated motions. An increase in the local motions, as reflected by the decrease in the rotational correlation times, was also observed with increasing temperature. The blue-shifted emission of lipid-conjugated probes **3** and **4** showed high fundamental anisotropy values (excitation at 470 nm, r_0 = 0.24 and 0.35, respectively) in LUVs compared to those of the red-shifted emission of complexes **1** (r_0 = 0.12), **2** (r_0 = 0.08), and **5** (r_0 = 0.12) in glycerol. The results of analyses of the time-resolved anisotropy data in terms of a double exponential decay for complexes **3** and **4** in LUVs at variable temperature are summarized in Table 2. At lower temperatures, the anisotropy decay revealed a significant contribution from the limiting anisotropy at infinite time (r_∞); a nonzero r_∞ is indicative of restricted motion

Table 2. Average Lifetime, Limiting Anisotropy, and Rotational Correlation Times for Complexes 3 and 4 in Egg-PC−LUVs (100 nm) from 5 to 50 °C

compound	temp (°C)	$\langle\tau\rangle^a$ (ns)	r_∞	θ_1 (ns)^b	θ_2 (ns)^b	χ^2
3	5	11	0.096	9.8(−1.62, 1.69)	2.46(−0.21, 0.24)	1.18
	10	9.4	0.07	8.62(−1.68, 2.4)	1.95(−0.18, 0.21)	1.10
	20	7.9	0.05	5.5(−1.31, 2.05)	1.2(−0.17, 0.18)	1.13
	30	6.7	0.03	4.1(−0.55, 0.68)	1.0(−0.06, 0.07)	1.19
	40	5.5	0.02	3.2(−1.84, 1.89)	0.58(−0.51, 1.0)	1.15
	50	4.5	0.01	1.6(−0.15, 0.42)	0.26(−0.06, 0.18)	1.14
4	5	7.2	0.09	8.4(−0.624, 1.2)	0.79(−0.21, 0.25)	1.19
	10	6.6	0.07	6.3(−0.54, 0.62)	0.83(−0.11, 0.13)	1.1
	20	5.8	0.04	5.4(−1.35, 2.01)	0.5(−0.03, 0.04)	1.2
	30	4.8	0.02	3.3(−0.15, 0.16)	0.36(−0.03, 0.02)	1.08
	40	3.8	0.01	2.0(−0.10, 0.11)	0.29(−0.04, 0.05)	1.0
	50	3.1	0.008	1.3(−0.08, 0.085)	0.13(−0.04, 0.041)	1.1

^{a}Intensity-averaged lifetime, $\langle\tau\rangle = \sum\alpha_i \tau_i^2/\sum\alpha_i \tau_i$. ^{b}The upper and lower 95% confidence limits, calculated by the support-plane method, are indicated within parentheses. Johnson, M. L.; Frasier, S. G. In *Methods in Enzymology*, Vol. 117, Academic Press: New York, 1985; p 301.

dx.doi.org/10.1021/ic400706u | *Inorg. Chem.* 2013, 52, 10835−10845

in the membrane.[32] Compound **7** was examined in DMPC−LUVs and showed a slightly longer lifetime of 4.56 ns, a very high fundamental anisotropy of 0.31, and a significant r_∞ of 0.103. These properties closely parallel those observed for complexes **3** and **4** in LUVs. The variable-temperature study of this emission showed very little variation in lifetime over the range of 0−30 °C, which is likely due to the low quantum yield observed for **7** in solution.

The absorption and emission spectra of cholesterol-conjugate complexes **5** and **9** in ethanol are shown in Figure 2. In contrast to the lipid-conjugate complexes **3** and **4**, the emission spectra of complexes **5** and **9** are red-shifted and identical to those observed when incorporated in the egg-PC−LUVs. In addition, the excited-state lifetimes 0.47 and 0.22 μs for **5** and **9** increased to 0.89 and 0.52 μs, respectively, for the complexes in egg-PC−LUVs at 23 °C in ethanol.

Complexes **4** and **7** both showed blue-shifted luminescence with a maximum near 505 nm and a lifetime of ∼4 to 5 ns in egg-PC−LUVs, similar to that observed in ethanol. This indicates that the large blue shifts and short lifetimes observed for the emissions of complexes **3** and **4** in LUVs are likely due to large perturbations in the geometry and/or electronic energies of the excited states.

In Complex **10** the lipid is conjugated to the phen rather than bpy ligand, which is the likely luminophore, does not show a blue shift, and has an excited state lifetime typical of a ^{3}MLCT (0.41 μs). The perturbations that result in the blue shifts and short lifetimes for complexes **3**, **4**, and **7** are likely the result of conjugation of the large lipid molecules directly to the luminophore or to an ancillary ligand (phosphines) that makes a significant contribution to the MLCT excited state, but this is not the case for complex **10**.[17,39]

Egg-PC has a low phase-transition temperature (less than 0 °C) because it contains mixed saturated and unsaturated acyl chains of different lengths, leading to a highly disordered phase. To understand the effect of a more ordered membrane on the observed rotational correlation times, we measured the photophysical properties of complex **5** incorporated in DPPC−LUVs, which have two 15-carbon saturated acyl chains. The phase-transition temperature for DPPC is 41 °C;[35] the bilayer is in an ordered phase below this temperature.

As in egg-PC, the emission of complex **5** was red-shifted in DPPC. An analysis of the time-dependent anisotropy decay of complex **5** incorporated in either egg-PC or DPPC−LUVs resulted in a fundamental anisotropy value of ∼0.1. A single exponential satisfactorily fit the time-resolved intensity decay of complex **5**. In the DPPC−LUVs, the luminescence lifetime of complex **5** ranges from 1.10 μs at 10 °C to 0.43 μs at 50 °C. This temperature range spans the phase-transition temperature of DPPC (41 °C). In egg-PC−LUVs, the same lifetime is comparable (0.96 μs at 10 °C and 0.45 μs at 50 °C) (see Figure 4). The long decay times suggest that these probes can be used to measure rotational motions as long as 3 μs (3 times the mean intensity decay time).[4,5]

The rotational motions of complex **5** in egg-PC−LUVs were also analyzed over a range of temperatures. The rotational correlation time decreased from 112 to 14 ns as the temperature increased from 10 to 50 °C (Table 3). The recovered rotational correlation times are not due to the overall rotation of the 100 nm diameter LUVs, which would cause these times to be much longer (sub-millisecond range), but are due to local motions. There is considerable uncertainty in measuring longer correlation times of the LUVs because of the difficulty of measuring

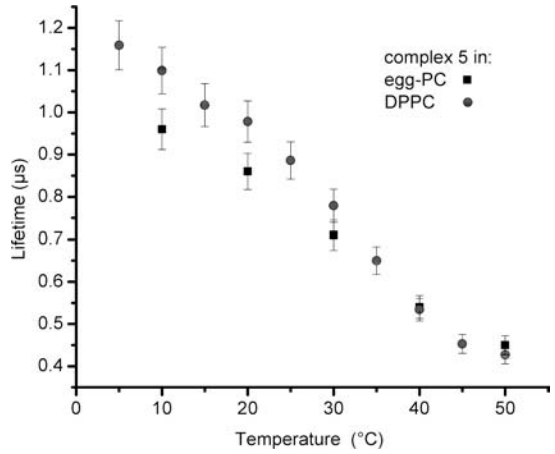

Figure 4. Average lifetime of complex [(H)Ru(CO)(dppene)(1,10-phen-5-NC(O)OChol)][PF_6] (**5**) in LUVs over a range of temperatures. Error bars are based on the errors in the nonlinear least-squares fit using the support plane method developed by M. L. Johnson and S. G. Frasier and described in *Methods in Enzymology*, Vol. 117, Academic Press: New York, 1985; p 301.

Table 3. Average Lifetime, Limiting Anisotropy, and Rotational Correlation Times for Complex 5 at a Range of Temperatures in 100 nm egg-PC−LUVs

temp (°C)	$\langle\tau\rangle^a$ (μs)	r_∞	ϕ (ns)^b	χ^2
5	1.46	0.058	71(−1.61, 2.0)	1.00
10	1.24	0.055	54(−1.47, 1.93)	1.02
20	0.94	0.046	49(−1.46, 2.0)	1.08
30	0.68	0.051	44(−1.51, 2.4)	1.08
40	0.57	0.049	24(−1.2, 2.27)	1.18
50	0.47	0.050	10(−4.21, 7.2)	0.98

[a]Intensity-averaged lifetime, $\langle\tau\rangle = \sum\alpha_i\tau_i^2/\sum\alpha_i\tau_I$. [b]The upper and lower 95% confidence limits, calculated by the support-plane method, are indicated within parentheses.

accurately a correlation time above 3 μs with a probe of 1 μs lifetime. Considering its luminescence lifetime, probe **5** would be more appropriate for studying the overall rotational motion of small unilamellar vesicles (SUVs) with diameters less than 20 nm, which have rotational correlation times in the sub-microsecond range. The time-dependent anisotropy decays at variable temperatures were analyzed by using single-exponential correlation times and a nonzero baseline limiting anisotropy (r_∞), which reflects the restricted motion of the probe during the lifetime of the excited state.[32,36−38]

One of the key design features of the series of complexes **1**−**7** was to decrease the molecular symmetry by using only one diimine ligand; we reasoned that the decreased symmetry would increase the excitation anisotropy of the transition-metal complex luminescence. To determine whether having only one diimine ligand in the cholesterol conjugate **5** has any significant effect on, or advantage for, the photophysical properties of this complex in membrane-like environments, we also synthesized, for comparison, a cholesterol derivative of complex **8**,[17,39] which contains three diimine ligands. This tris-diimine cholesterol conjugate, **9**, had a ^{1}MLCT absorption band and a red-shifted emission maximum similar to those of conjugate **5** (see Figure 2). The tris-diimine complex **9** also had a similar luminescence lifetime (∼0.41 μs at 20 °C when incorporated in egg-PC−LUVs). However, the fundamental luminescence anisotropy was much smaller (with excitation at 470 nm, $r_0 \approx 0.02$ for complex **9**

dx.doi.org/10.1021/ic400706u | *Inorg. Chem.* 2013, 52, 10835−10845

versus $r_0 \approx 0.12$ for complex **5**), consistent with the hypothesis that the larger fundamental luminescence anisotropy of the cholesterol conjugate **5** is due to the decreased symmetry of the monodiimine complex. The anisotropies of the parent complexes **1** and **2** are similar to those of complex **5**.

DISCUSSION

The ruthenium probes reported in this paper that were synthesized with only one diimine ligand showed both the long, microsecond excited-state lifetimes and the sufficiently high fundamental anisotropies required to study dynamics in the submicrosecond−microsecond time range. Interestingly, the lipid conjugates showed no emission in the case of complex **3** and short-lived blue-shifted emissions in the cases of complexes **4** and **7**, in alcohol or chloroform. This lack of emission is likely due to the large number of vibrational modes available, which increases the nonradiative decay when the conjugates are in organic solvents. Consistent with this, conjugate **3**, which has two lipids, was nonemissive, whereas conjugate **4**, which has only one lipid and the more rigid phenanthroline ring, showed a weak emission that was blue-shifted and short-lived. Interestingly, conjugate **7**, in which the lipid is conjugated to the phosphine, showed a blue-shifted weak emission that had a short lifetime in solution; this is likely the result of perturbation of the orbitals contributing to the MLCT excited state or energy transfer to intraligand transitions.[25] In the more constrained environment of the PC−LUVs, intense blue-shifted emissions were observed for complexes **3** and **4**. Complex **7** showed a similar blue shift but with lower intensity in both the LUVs and the organic solvents. Furthermore, the fact that the MLCT absorption spectra of complexes **3**, **4**, and **7** are very similar in solution and in the LUVs indicates that the orbital perturbation resulting in the blue shift must occur only in the excited state after the electron is transferred from the metal center to the aromatic ring. This suggests that in the initial excited state, the orbital energies are perturbed such that emission takes place from a singlet π^* state. Similar effects have been observed in other ruthenium complexes.[25] Consistent with this interpretation, they also have very short excited-state lifetimes relative to the parent complexes, as well as much higher fundamental anisotropies (see Table 2); the photophysical properties—Stokes shift and lifetime—observed for complexes **3**, **4**, and **7** in lipid LUVs are characteristic of a singlet emission, although a short-lived triplet cannot be strictly ruled out. Note that the previously reported tris-diimine lipid-conjugated complex **10** does not show the anomalous blue-shifted, short-lived emissions observed for complexes **3**, **4**, and **7**. This could be because, in this complex, the unsubstituted diimine ring is the electron acceptor from the metal, and the lipid-conjugated phenanthroline ligand makes no contribution to the excited state, whereas in complexes **3**, **4**, and **7** the phosphine ligand does contribute to the excited state. This is borne out by the excitation spectra for complexes **3**, **4**, and **7**, in which a significant contribution from phosphine absorptions is observed at about 325−350 nm (see Supporting Information).

We considered the possibility that the anomalous blue shifts could be due to a fluorescent impurity. However, excitation at varying wavelengths within the MLCT band results in identical emission line shapes characteristic of that compound, and the intensity varies, as expected for the differences in absorption at the different excitation wavelengths. This confirms that the spectra are not due to an impurity.

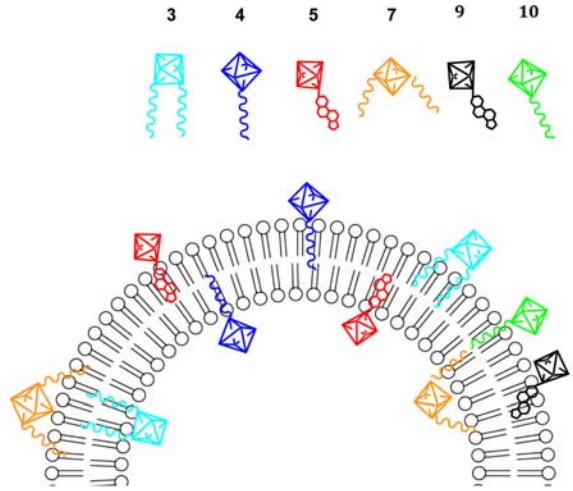

$[HRu(CO)(PPh_3)_2(dcbpy\text{-}N\text{-}DPPE_2)][PF_6]$ (**3**)

[HRu(CO)(dppene)(1,10-phen-5-NHC(S)-*N*-DPPE)][PF_6] (**4**)

$HRu(CO)(dppene)(1,10\text{-}phen\text{-}5\text{-}NHC(O)OChol)][PF_6]$ (**5**)

$HRu(CO)(PhP_2C_2H_4C(O)\text{-}N\text{-}DPPE)_2(bpy)][PF_6]$ (**7**)

$HRu(bpy)_2(1,10\text{-}phen\text{-}5\text{-}NHC(O)OChol)][PF_6]_2$ (**9**)

$HRu(bpy)_2(1,10\text{-}phen\text{-}5\text{-}NHC(S)\text{-}N\text{-}DPPE)][PF_6]_2$ (**10**)

Figure 5. Representation of the MLC−LUV conjugate interactions showing the differences in probe incorporation into the lipid bilayer.

Accompanying the short excited-state lifetimes (11 and 8 ns) in LUVs, the lipid conjugates have high fundamental anisotropy and temperature-sensitive rotational correlation times, which are helpful for studying faster, local motions (up to 33 ns) in the LUVs. Complexes **3** and **4**, which have two and one lipid conjugate, respectively, have double exponential anisotropy decays when incorporated in LUVs. Interestingly, the longer rotational correlation decay times are similar (7−8 ns at 10 °C, Table 2). Both the time scale and the insensitivity to the number of lipid anchors suggest that this motion reflects restricted diffusion, classically referred to as "wobble-in-a-cone,"[36−38] and is not due to axial rotation.[40]

In the wobble-in-a-cone model, it is assumed that the major axis of the probe wobbles randomly within a cone of semiangle θ_c, which can be estimated using the following relationship:

$$\frac{r_\infty}{r_0} = \left[\frac{1}{2}\cos\theta_c(1+\theta_c)\right]^2 \qquad (2)$$

The temperature-dependent motions of the lipid probes in egg-PC−LUVs were analyzed using this model. Over the temperature range from 10 to 50 °C, the cone angle θ_c varied from 44° to 72° for complex **3** and from 55° to 74° for complex **4**. In contrast to the longer correlation times, the shorter correlation times are significantly different for complexes **3** and **4** (2.0 and 0.7 ns, respectively at 10 °C, Table 2). This time scale and the dependence on the number of anchoring lipids indicate that these shorter rotational correlation times mainly reflect the diffusive dynamics of the probe-labeled headgroup.[40] Thus, these probes could be useful for studying lipid-headgroup motions.

Recently, reversible coordination and lipid incorporation of a Ru(II) diimine−aqua complex to a thioether cholesteryl conjugate that was previously incorporated into lipid vesicles was

dx.doi.org/10.1021/ic400706u | *Inorg. Chem.* 2013, 52, 10835−10845

reported.[41] Complex **5**, however, to our knowledge, represents the first cholesterol conjugate covalently linked to the diimine ring. The long excited-state lifetimes relative to fluorescence (microseconds versus nanoseconds) and high anisotropy values observed for probe **5** in glycerol and in PC−LUVs make this probe an excellent candidate for studying membrane dynamics on the microsecond time scale. That the cholesterol probes do not show the blue shifts observed for the lipid probes is likely related to the greater rigidity of the cholesterol molecule, and this structural feature leads to less perturbation of the excited-state orbitals. Preliminary data from our laboratory[42] show that this probe is useful for studying the global dynamics of lipid nanodiscs, which are 10 nm diameter recombinant lipoprotein A-lipid constructs.[43]

CONCLUSIONS

Three ruthenium-based luminescent bioconjugates with only one diimine ligand have been designed and synthesized as membrane probes. The steady-state and time-dependent photophysical properties of these complexes were studied in solution and in model membrane environments, in which the probes were distributed between the inner and outer leaflets (see Figure 5). An important part of the design of the conjugates was the use of phosphine ligands, which have previously been shown to improve luminescence quantum yields.[18,19] Lipid conjugates **3**, **4**, and **7** showed unexpectedly blue-shifted, relatively intense emissions with short, nanosecond-time scale luminescence lifetimes in solution and in the LUVs. In the LUVs these emissions were sensitive to changes in membrane viscosity. These complexes would not be useful for studying the microsecond-time scale dynamics on membranes, but could be useful for nanosecond-time scale processes. These results sharply contrast with the previously reported tris-diimine lipid conjugates, which exhibited the typical red-shifted, long-lived emissions.[2,17] Complexes **5**, **9**, and **10** could be used as probes for studying the slower dynamics. Our results point to the sensitivity of the transition-metal complex−lipid interaction to the ancillary ligands of the complex. A similar blue shift and short decay time were recently observed for the related complex $[Ru(bpy)_2(dpp)]^{2+}$ (dpp = 2,3-bis(2-pyridyl)pyrazine) upon protonation of the pyrazine nitrogen.[44] This suggests that these blue shifts are due to perturbations in the orbital energies of the diimine ligand, and this suggestion is further supported by the absence of the blue shift in complexes **9** and **10**. The cholesterol conjugate **5** incorporated in phosphatidylcholine LUVs had lifetime and anisotropy decays that were sensitive to temperature-dependent motions, and conjugation to cholesterol did not significantly perturb the fundamental anisotropy. In addition, the comparison with the tris-diimine cholesterol conjugate **9** revealed that having only one diimine results in a greater fundamental luminescence anisotropy.

In summary, the unusual behavior of lipid conjugates **3**, **4**, and **7** relative to complex **10** points to the importance of the phosphine ligands in controlling photophysical properties via their contribution to the excited state electron distribution when present in combination with multiple vibrational modes of the attached lipids. These contributions are not apparent in the excitation spectra of complexes **8**−**10** (see Figure 3 and Supporting Information).[17]

ASSOCIATED CONTENT

Supporting Information

Details of the methods used for obtaining time-resolved luminescence spectra, the synthesis of the bis-lipid conjugate of bpy (**11**), NMR, excitation, and absorption spectra for complexes **1**−**9**. This material is available free of charge via the Internet at http://pubs.acs.org.

AUTHOR INFORMATION

Corresponding Authors

*E-mail: edward.rosenberg@mso.umt.edu (E.R.).
*E-mail: sandy.ross@umontana.edu (J.B.A.R.).

Present Address

[§]Author is presently at CIC biomaGUNE but was at the University of Montana when the project started. E-mail: lsalassa@cicbiomagune.es.

Notes

The authors declare no competing financial interest.

ACKNOWLEDGMENTS

We gratefully acknowledge the National Science Foundation (CHE-0709738 and CHE-1049569) and the National Institutes of Health National Center for Research Resources (P20 RR15583 and P20 GM103546) for the generous support of this research. We thank Labe Black for help with the luminescence spectroscopy.

REFERENCES

(1) Szmacinski, H.; Terpetschnig, E.; Lakowicz, J. R. *Biophys. Chem.* **1996**, *62*, 109.
(2) (a) Li, L.; Szmacinski, H.; J. R. Lakowicz, J. R. *Anal. Biochem.* **1997**, *244*, 80. (b) Li, L.; Szmacinski, H.; J. R. Lakowicz, J. R. *Biospectroscopy* **1997**, *3*, 155.
(3) Li, L.; Szmacinski, H.; J. R. Lakowicz, J. R. *Biospectroscopy* **1997**, *3*, 155.
(4) Johnson, P.; Garland, P. B. *Biochem. J.* **1982**, *203*, 313.
(5) Lakowicz, J. R. *Principles of Fluorescence Spectroscopy*, 3rd ed.; Springer: New York, 2006.
(6) Dadak, V.; Vanderkooi, J. M.; Wright, W. W. *Biochim. Biophys. Acta* **1992**, *110*, 33.
(7) Bartholdi, M.; Barrantes, F. J.; Jovin, T. M. *Eur. J. Biochem.* **1981**, *120*, 389.
(8) Che, A.; Cherry, R. J. *Biophys. J.* **1995**, *68*, 1881.
(9) Klug, C. S.; Feix, J. B. *Methods Cell Biol.* **2008**, *84*, 617−658.
(10) (a) Chi, Y.; Chou, P.-T. *Chem. Soc. Rev.* **2007**, *36*, 1421. (b) Piszczek, G. *Arch. Biochem. Biophys.* **2006**, *453*, 54.
(11) Sharmin, A.; Darlington, R. C.; Hardcastle, K. I.; Ravera, M.; Rosenberg, E.; Ross, J. B. A. *J. Organomet. Chem.* **2009**, *694*, 988.
(12) Kober, E. M.; Sullivan, B. P.; Dressick, W. J.; Caspar, J. V.; T., J.; Meyer, T. J. *J. Am. Chem. Soc.* **1980**, *102*, 7383.
(13) Chen, P.; Meyer, T. J. *Chem. Rev.* **1998**, *98*, 1439.
(14) Shan, B.-Z.; Zhao, Q.; Goswami, N.; Eichorn, D. M.; Rillema, D. P. *Coord. Chem. Rev.* **2001**, *211*, 117.
(15) Stufkens, D. J.; Vleek, A., Jr. *Coord. Chem. Rev.* **1998**, *177*, 127.
(16) Terpetschnig, E.; Szmacinski, H. M.; Lakowicz, J. R. *Biophys. J.* **1995**, *68*, 342.
(17) (a) X. Guo, L. Li; F. N. Castellano, H.; Szmacinski, H.; Lakowicz, J. R. *Anal. Biochem.* **1997**, *254*, 179. (b) Guo, X.-Q.; Castellano, F. N.; Li, L.; Lakowicz, J. R. *Biophys. Chem.* **1998**, *71*, 51.
(18) Kober, E. M.; Meyer, T. J. *Inorg. Chem.* **1983**, *22*, 1614.
(19) Kober, E. M.; Meyer, T. J. *Inorg. Chem.* **1984**, *23*, 3877.
(20) Caspar, J. V.; Meyer, T. J. *J. Phys. Chem.* **1983**, *87*, 952.
(21) Freed, K. F. *Acc. Chem. Res.* **1978**, *11*, 74.
(22) Kober, E. M.; Marshall, J. L.; Dressick, W. J.; Sullivan, B. P.; Casper, J. V.; Meyer, T. J. *Inorg. Chem.* **1985**, *24*, 2755.
(23) Kober, E. M.; Casper, J. V.; Lumpkin, R. S.; Meyer, T. J. *J. Phys. Chem.* **1986**, *90*, 3722.
(24) Boyde, S.; Strouse, G. F.; Jones, W. E.; Meyer, T. J. *J. Am. Chem. Soc.* **1990**, *112*, 7395.
(25) Balaz, G. C.; Gurezo, G. C.; Schmehl, R. H. *Photochem. Photobiol. Sci.* **2005**, *4*, 89.

(26) Treadway, J. A.; Loeb, B.; Lopez, R.; Anderson, P. A.; Keene, F. R.; Meyer, T. J. *Inorg. Chem.* **1996**, *35*, 2242.
(27) Garino, C.; Ghiani, S.; Gobetto, R.; Nervi, C.; Salassa, L.; Ancarani, V.; Neyroz, P.; Franklin, L.; Ross, J. B. A.; Seibert, E. *Inorg. Chem.* **2005**, *44*, 3875.
(28) Li, L.; F. N. Castellano, F. N.; Gryczynski, I.; Lakowicz, J. R. *Chem. and Phys. of Lipids* **1999**, *99*, 1.
(29) Gobetto, R.; Caputo, G.; Garino, C.; Ghiani, S.; Nervi, C.; Salassa, L.; Rosenberg, E.; Ross, J. B. A.; Viscardi, G.; Martra, G. *Eur. J. Inorg. Chem.* **2006**, No. 14, 2839.
(30) (a) Parker, C. A. *Photoluminescence of Solutions with Applications to Photochemistry and Analytical Chemistry*; Elsevier: Amsterdam, 1968; p 262. (b) Kellogg, R. E.; Bennett, R. G. *J. Chem. Phys.* **1964**, *41*, 3042.
(31) Barkley, M. D.; Kowalczyk, A. A.; Brand, L. *J. Chem. Phys.* **1981**, *75*, 3581.
(32) Dale, R. E.; Chen, L. A.; Brand, L . *J. Biol. Chem.* **1977**, *252*, 7500.
(33) Badea, M. G.; Brand, L. *Methods Enzymol.* **1979**, *61*, 378.
(34) Paoletti, J.; Le Pecq, J. B. *Anal. Biochem.* **1969**, *31*, 33.
(35) (a) Avanti Polar Lipids Technical Support Liposome Preparation page. Preparing Large, Unilamellar Vesicles by Extrusion (LUVET). http://avantilipids.com/index.php?option=com_content&=article&id=1600&Itemid=381 (accessed March 1, 2013). (b) Kim, J.-C.; Bae, S. K.; Kim, J.-D. *J. Biochem.* **1997**, *121*, 15.
(36) Kinosita, K., Jr.; Kawato, S.; Ikegami, A. *Biophys. J.* **1977**, *20*, 289.
(37) Kinosita, K., Jr.; Ikegami, A.; Kawato, S. *Biophys. J.* **1982**, *37*, 461.
(38) Minazzo, A. S.; Darlington, R. C.; Ross, J. B. A. *Biophys. J.* **2009**, *96*, 681.
(39) Youn, H. J.; Terpetschnig, E.; Szmacinski, H.; Lakowicz, J. R. *Anal. Biochem.* **1995**, *232*, 24.
(40) Klauda, J. B.; Roberts, M. F.; Redfield, A. G.; Brooks, B. R.; Pastor, R. W. *Biophys. J.* **2008**, *94*, 3074.
(41) Bonnet, S.; Limburg, B.; Meeldijk, J. D.; Klein-Gebbink, R. J. M.; Killian, J. A. *J. Am. Chem. Soc.* **2011**, *133*, 252.
(42) Black, L. A.; Rosenberg, E.; Sharmin, A.; Ross, J. B. A. American Chemical Society, Northwest Regional Meeting, June 26−29, 2011; *Poster 169*.
(43) Nath, A.; Atkins, W. M.; Sligar, S. G. *Biochemistry* **2007**, *46*, 2059.
(44) Zambrana, J. L., Jr.; Ferloni, E. X.; Colis, J. C.; Gafney, H. D. *Inorg. Chem.* **2008**, *47*, 2.